DOI: 10.1002/ejic.200900509

Mixed-Linker Metal-Organic Frameworks as Catalysts for the Synthesis of Propylene Carbonate from Propylene Oxide and CO_2

Wolfgang Kleist,[a] Fabian Jutz,[a] Marek Maciejewski,[a] and Alfons Baiker*[a]

Keywords: Carbon dioxide / Coordination polymers / Metal–organic frameworks / Propylene carbonate / Heterogeneous catalysis

A series of mixed-linker metal-organic frameworks (MIXMOFs) of the general formula $Zn_4O(BDC)_x(ABDC)_{3-x}$ has been synthesized and tested as catalyst in the reaction of propylene oxide (PO) and carbon dioxide. Based on MOF-5 a new synthetic route was developed which allows the partial substitution of benzene-1,4-dicarboxylate (BDC) linkers in the material by functionalized 2-aminobenzene-1,4-dicarboxylate. In that way the number of catalytically active amino groups can be tuned using the desired BDC/ABDC ratio. The presence of MIXMOFs (instead of a mechanical mixture of MOF-5 and IRMOF-3) was proven by high-resolution X-ray diffraction and DTG. XRD and TG/MS analysis revealed that pure MIXMOF materials can be obtained up to an ABDC loading of 40 %. The thermal stability in air is decreasing with increasing ABDC content from 450 °C for pure MOF-5 (0 % ABDC) to ca. 350 °C for the 40 % MIXMOF $Zn_4O(BDC)_{1.8}(ABDC)_{1.2}$. Consequently, MIXMOF materials represent a promising class of materials for catalytic applications in the temperature range at least up to 300 °C which is proven using the synthesis of propylene carbonate (PC) from propylene oxide and carbon dioxide as a test reaction. The catalytic results indicate that solid MIXMOF catalysts in combination with tetraalkylammonium halides (NR_4X) as promoters are as active as the corresponding homogeneously dissolved reference compounds (H_2ABDC, H_2BDC and Zn salts) and that they can be recycled with only moderate loss in activity. A comparison of MIXMOFs from 0 to 40 % of ABDC revealed a dependence of activity on the number of amino groups. Due to the fact that even pure MOF-5 catalyzed the reaction to some extent, surface Zn centers with free coordination sites might also contribute to substrate activation. Using optimized reaction conditions, a PC yield of up to 63 % can be obtained after 3 h in the presence of low catalyst concentration (0.045 mol-% of 40 % MIXMOF, containing 0.05 mol-% of NH_2 groups).

Introduction

Due to their beneficial properties metal-organic frameworks (MOFs) or porous coordination polymers (PCPs) have in recent years become an interesting class of materials in various fields of chemistry.[1] By now a huge variety of bi- or multifunctional organic linker molecules and transition metal units have been applied as building blocks leading to numerous microporous 3-D structures featuring extremely high specific surface areas and pore volumes.[2–6] While the field of possible applications was in the beginning limited to storage of hydrogen or light hydrocarbons,[7–9] the scope was soon extended to other fields, such as sensor techniques[10,11] and gas purification or separation.[12,13] Another promising field which is currently investigated by various groups concerns the implementation of MOFs in heterogeneous catalysis.[14] Since many of the MOF structures suffer from a low thermal stability or are extremely sensitive (towards air, acids, bases, water or common organic solvents), one major challenge here is the proper choice of framework materials which exhibit sufficient stability under typical reaction conditions. Another important aspect concerns the introduction of catalytically active sites. Up to now three different methodologies have been proposed in the literature.

(i) In the first approach, frameworks are built from metal centers which should act as the catalytically active sites themselves.[15,16] Hence it is crucial that free coordination sites are available at these metal centers; otherwise a coordination of substrate molecules would be either impossible or lead to a dissolution and decomposition of the framework. In addition, MOFs which are built from, e.g., palladium exhibit a very high (stoichiometric) amount of the noble metal.

(ii) As an alternative, several groups presented strategies in which metallic nanoparticles have been introduced to the pore system. This can be achieved by either solution infiltration[17] or vapor deposition techniques.[18,19] However, in some cases a dramatic decrease of the specific surface area has been observed due to blocking of the pores and chan-

[a] Department of Chemistry and Applied Biosciences, Institute for Chemical and Bioengineering, ETH Zürich
Hönggerberg HCI, 8093 Zürich, Switzerland
Fax: +41-44-63-21163
E-mail: baiker@chem.ethz.ch

Supporting information for this article is available on the WWW under http://dx.doi.org/10.1002/ejic.200900509.

nels. Another question might be whether the noble metal particles are really deposited inside the pores or whether they are (at least partially) located at the outer surface as indicated in some cases (e.g. for Au@MOF-5)[18] when the metal particle size was larger than the pore diameter of the MOF.

(iii) Finally, active centers have been introduced into metal-organic frameworks using functional side groups of the linker molecules. These organic groups might either act as the active sites themselves or they can be modified with further functionalities via postsynthetic treatment techniques.[20–22] Another possibility is that such functional groups act as "surface ligands" which can be used to immobilize catalytically active transition metals.[23–26] The problem of a stoichiometric loading of the resulting catalyst can be overcome by using mixed-linker metal-organic frameworks.[27] In this approach two isoreticular linker molecules, one with an additional functional side group, the other without, are randomly distributed in the framework leading to a mixed structure in which the number of active sites is tunable by choosing the required ratio of the two linker molecules.

In this work we present a series of MIXMOF materials (see Scheme 1 and Figure 1) which are based on MOF-5 and the corresponding IRMOF series.[2] The benzene-1,4-dicarboxylate linkers have been partially (from 0 to 90%) substituted by 2-aminobenzene-1,4-dicarboxylate as the functionalized linker bearing an amino side group which can act as a weak basic site in catalysis.

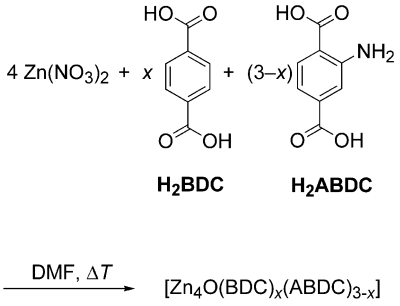

Scheme 1. Synthesis of mixed-linker metal-organic frameworks (MIXMOFs) containing variable ratios of benzene-1,4-dicarboxylate (BDC) and 2-aminobenzene-1,4-dicarboxylate (ABDC) linkers.

As a test reaction we have chosen the formation of propylene carbonate (PC) by insertion of carbon dioxide into propylene oxide (PO, see Scheme 2) which is of great industrial interest, because cyclic carbonates have found application as green solvents or electrolytes in lithium ion batteries. In addition, they represent important intermediates in fine chemical synthesis and polymerization. The present reaction route via CO_2 fixation is attractive due to the fact that carbon dioxide represents a cheap, clean and non-toxic carbon source (in contrast to e.g. carbon monoxide, phosgene, or isocyanates).[28,29]

Consequently, a variety of different catalyst systems has been applied in this type of reaction up to now. In homogeneous catalysis a wide range of different transition metal

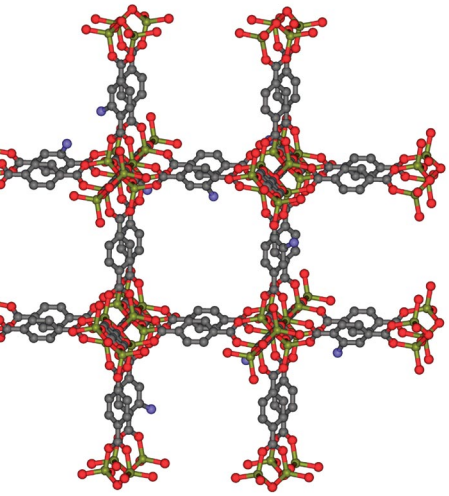

Figure 1. Structure of MOF-5 based mixed-linker metal-organic framework (MIXMOF). Benzene-1,4-dicarboxylate (BDC) linkers have been partially substituted by 2-aminobenzene-1,4-dicarboxylate (ABDC). Zn atoms are displayed in yellow, O in red, C in grey and N in blue.

Scheme 2. Catalytic test reaction: formation of propylene carbonate (PC) via insertion of CO_2 into propylene oxide (PO) in the presence of MIXMOF catalysts and tetraalkylammonium halides as promoters.

complexes have been used. Especially salen, phthalocyanin or porphyrin complexes of transition metals (e.g. Cr,[30] Co[31,32] Ni,[33] Cu,[31] Zn[31,34]) or main group elements such as aluminum[35,36] or tin[37] were found to be highly active. Coordination of the epoxide at the metal center via its oxygen atom is generally assumed to be the first step of the catalytic cycle. However, in most cases additional promoters like tetraalkylammonium halides are needed.[38,39] Also ionic liquids were successfully applied as catalysts or promoters in combination with transition metal salts.[40,41] Most probably, the anions of these compounds facilitate a ring opening of the coordinated epoxide which is then accessible for the CO_2 insertion.[42]

To overcome the problems of catalyst separation with these systems, efforts in the application of heterogeneous catalysts have been undertaken. One main strategy concerned the immobilization of homogeneous catalysts onto solid supports,[30,34,43,44] but also metal oxides, like ZnO/SiO_2[45] or MgO,[46] catalyzed the reaction. In addition, porous materials like MCM-41,[47] Cs zeolites[48] or amine-functionalized Ti(Al)-SBA-15[49] were used. In the latter case the authors claimed a modified reaction mechanism including an activation of carbon dioxide at the amino groups of the functionalized surface. According to the proposed mechanism, a nucleophilic attack of the amino group at the carbon atom of CO_2 will lead (via a carbamate intermediate) to an "activated CO_2" in form of carbamic acid

which can further react with the epoxide. Based on this finding we concluded that our MIXMOFs bearing also amino groups might be a promising class of materials for the chosen test reaction.

Results and Discussion

Material Synthesis and Characterization

A series of MIXMOF materials $Zn_4O(BDC)_x(ABDC)_{3-x}$ was synthesized in which the 1,4-benzenedicarboxylate (BDC) linkers are substituted partially by 2-aminobenzene-1,4-dicarboxylate (ABDC, see Scheme 1). The synthesis is performed in a round-bottom flask under ambient pressure. To allow for a random distribution of the two linker molecules, no additional base is added. Otherwise slow addition of the base would most probably lead to a selective deprotonation of the stronger acid first, resulting finally in core-shell particles. Reaction conditions were found to be crucial to obtain a phase-pure material. SEM pictures presented in Figure 2 indicate the formation of cubic particles of several micrometer size (top) which form large agglomerates (bottom) for both pure MOF-5 (left) and 40% MIXMOF (right). At a reaction temperature of 150 °C up to 90% of ABDC linkers could be introduced to the MIXMOFs.

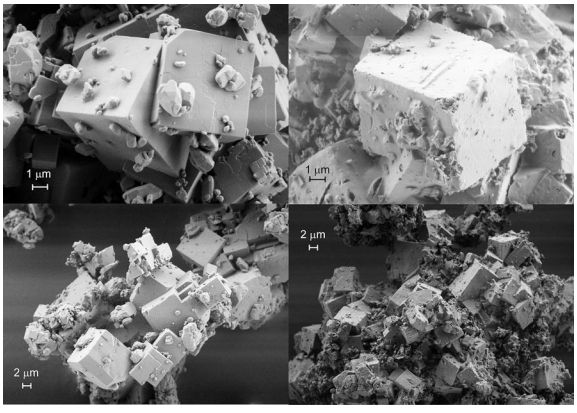

Figure 2. SEM pictures of MOF-5 (0% of ABDC, left) and 40% MIXMOF (right) indicating the formation of cubic particles (top) which form larger agglomerates (bottom).

The corresponding X-ray powder diffraction patterns are shown in Figure 3. Since the single crystal data for MOF-5 (100% BDC; $x = 3$) and IRMOF-3 (100% ABDC; $x = 0$) are very similar, it seems to be obvious that the powder patterns of both pure materials and our samples with mixed structures should be more or less identical. Consequently, all peaks observed for the series from 0 to 90% of ABDC content are in accordance with simulated patterns calculated from the single crystal data. Note that crystallinity was strongly decreasing at a high ABDC content of 90%, finally leading to a more or less amorphous structure at 100% substitution. Obviously, the synthesis of pure IRMOF-3 is not possible under the chosen reaction conditions.

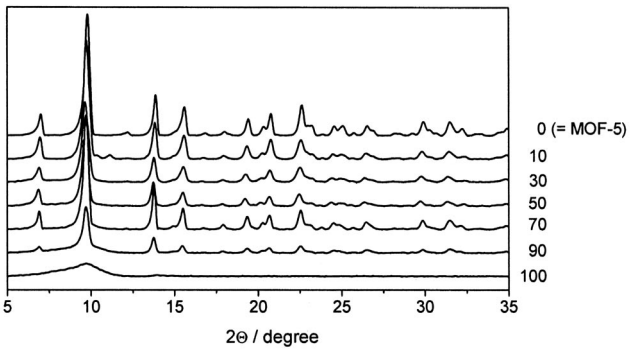

Figure 3. X-ray powder diffraction patterns of the MIXMOF series. The molar percentage of ABDC linkers is marked on the corresponding curves.

Due to the identical XRD patterns which would be expected for pure MOF-5, IRMOF-3 and the series of MIXMOFs it is impossible to prove the presence of materials with randomly distributed linker molecules using conventional X-ray diffraction. In order to exclude the possible formation of pure, separated phases of MOF-5 and IRMOF-3 we performed high-resolution X-ray diffraction experiments using synchrotron radiation. The results presented in Figure 4 show a clear linear shift of the peak positions from MOF-5 to the higher substituted MIXMOFs, which should be expected for materials with a random distribution of the two linker molecules according to Vegard's law. A mechanical mixture of MOF-5 and IRMOF-3 should, in contrast, lead to a splitting into two peaks at 2Θ values of ca. 3.13 (MOF-5) and 3.14 (IRMOF-3), respectively, which was not observed. Note that the absolute peak position at a 2Θ value of ca. 3.13 is shifted (compared to the position at a 2Θ value of ca. 9.75 in Figure 3) due to the different wavelength of the X-rays in the high-resolution experiment.

Further evidence for the presence of real MIXMOFs (instead of a mechanical mixture) results from combined TG-MS studies in an oxidizing atmosphere (20 vol.-% O_2 in He). The thermogravimetric curves presented in Figure 5 (top left) indicate clearly that with increasing amount of ABDC the thermal stability of the resulting material is successively decreasing. While the pure MOF-5 (0% of ABDC) is thermally stable under these conditions up to a temperature of at least 450 °C, decomposition of the mixed-linker MOFs starts at temperatures of ca. 400 °C for the 10% MIXMOF or even 350 °C for materials with a higher ABDC/BDC ratio. In accordance to this observation peak maxima of the MS signals for the masses $m/z = 78$ (benzene, top right), 44 (CO_2, bottom left) and 73 (DMF, bottom right) during the decomposition/combustion of the materials are shifted to lower temperatures with increasing ABDC content. Note that in all cases traces of the residual DMF solvent were present in the materials which could not be removed from the material before decomposition starts.

The decrease of the thermal stability is clearly demonstrated by evaluation of the corresponding DTG curves (first derivative of TG) which are presented in Figure 5

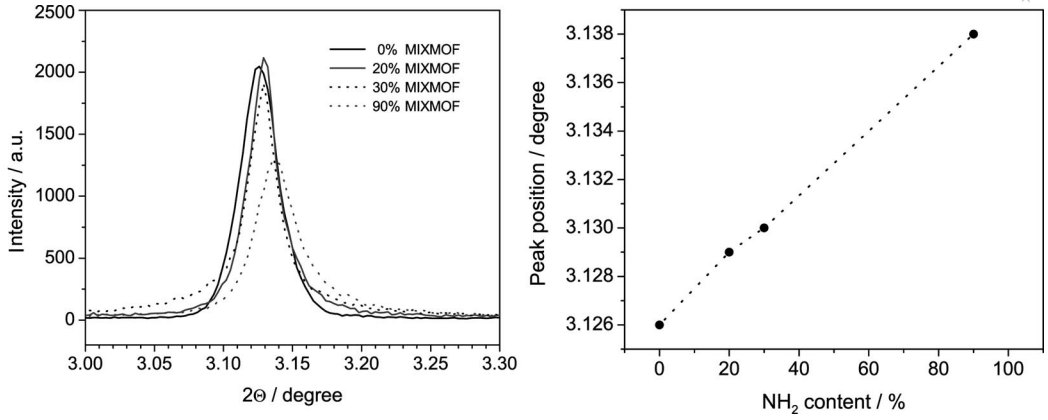

Figure 4. Peak shift of the MIXMOF series observed using high-resolution X-ray diffraction. Partial substitution of BDC linker molecules by ABDC leads to a slightly contracted unit cell, which is displayed by a linear correlation of ABDC content and peak shift to higher 2Θ values.

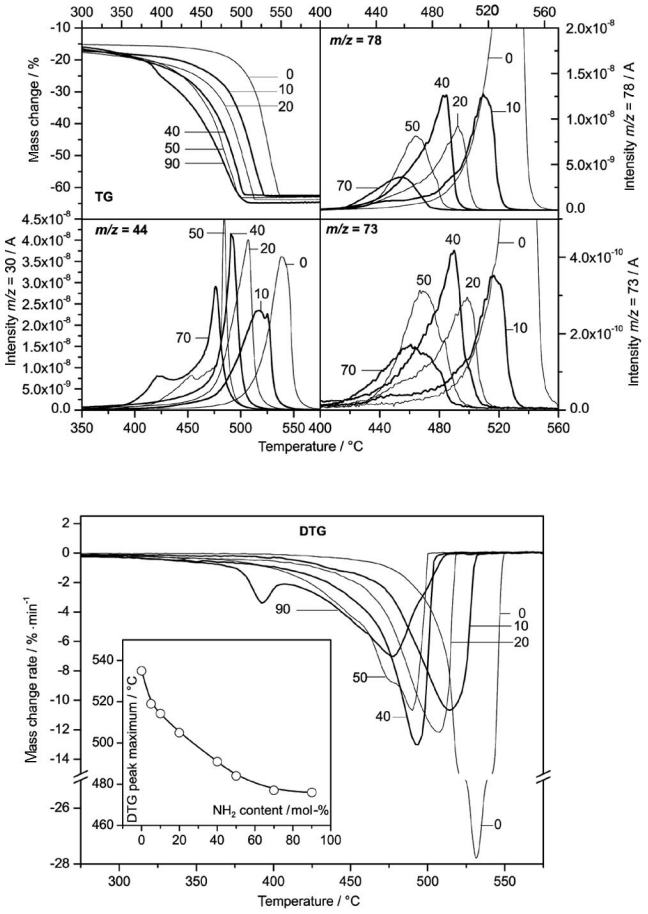

Figure 5. TG, MS (top) and DTG (bottom) data of the MIXMOF series, obtained in an oxidizing atmosphere (20 vol.-% O_2 in He). TG, MS (CO_2 m/z = 44, DMF m/z = 73, benzene m/z = 78) and DTG signals show a decreased thermal stability with increasing ABDC content which is confirmed by a shift of MS and DTG peak maxima towards lower temperatures. Note that a second maximum is observed in the DTG plots for materials with an ABDC content > 40% which indicates the formation of an additional phase.

(bottom). As can be seen from the plot in the Figure inset, the peak maxima in the DTG curves (representing the highest rate of decomposition) are shifted from 535 °C for pure MOF-5 to ca. 480 °C for the highly substituted 70 and 90% MIXMOFs. The shape of the DTG graphs provides additional information. For the materials from 0 to 40% ABDC only one maximum can be found which clearly indicates the presence of only one phase containing a mixture of both linker molecules. If pure MOF-5 and IRMOF-3 would be formed, two peaks, characteristic for the two compounds, should be expected with different intensities depending on the ABDC/BDC ratio. This has been proven in an according experiment, where we investigated a mechanical mixture of MOF-5 and the amorphous material that was obtained with 100% of ABDC under the chosen reaction conditions in the TG system. The results are presented in Figure S1 in the Supporting Information

Due to the fact that we observe additional peak maxima in the materials with higher ABDC loading (starting from 50%), we suppose that the formation of phase-pure MIXMOFs can only be achieved for an ABDC content ≤ 40%. A similar observation has been made in Raman studies (see Figure S2 in the Supporting Information). Consequently, we used the 40% MIXMOF $Zn_4O(BDC)_{1.8}$-$(ABDC)_{1.2}$ as the standard material in the catalytic tests.

All important results of the TG-MS study for this material are summarized in Figure 6. A first mass loss can be observed in the TG and DTG plots in the temperature range from ca. 100 to 300 °C (Figure 6, A). Although the material was pre-dried at 80 °C in vacuo to remove physically adsorbed solvent, DMF (m/z = 73) is evolved from the pore structure in the corresponding temperature range causing a total mass loss of 16.7 wt.-%. Decomposition/combustion of the material starts at comparatively high temperatures confirmed by a DTG maximum of 491 °C. The total mass loss of 62.5 wt.-% is in accordance with the expected formation of ZnO as the final product. During the thermal decomposition small amounts of remaining DMF

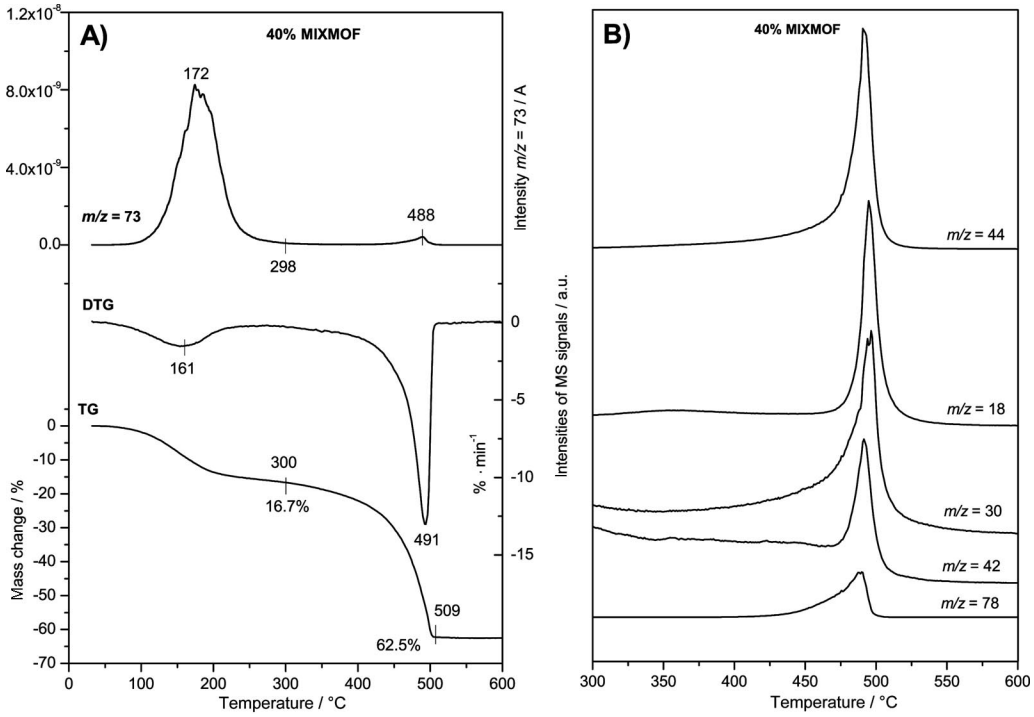

Figure 6. TG/MS traces recorded during decomposition/combustion of the standard catalyst (40% MIXMOF) in 20 vol.-% O_2. A) TG, DTG and MS: *m*/*z* = 73 (strongest signal of DMF); B) MS spectra of CO_2 (*m*/*z* = 44), water (*m*/*z* = 18), DMF (*m*/*z* = 42 and 30), NO (*m*/*z* = 30) and benzene (*m*/*z* = 78).

solvent are evolved (see the maximum on the *m*/*z* = 73 signal centered at 488 °C in Figure 6, A), while most of the mass loss is combined with the evolution of CO_2 (*m*/*z* = 44), H_2O (*m*/*z* = 18), and benzene (*m*/*z* = 78). The two signals for *m*/*z* = 30 and 42 represent the fragmentation and combustion of DMF (Figure 6, B).

In addition to the peak shift of the DTG curves, the increasing amount of ABDC linkers incorporated into the MIXMOF structures is also confirmed by MS data. During the decomposition of the material NO (*m*/*z* = 30) is formed by oxidation of the amino side groups of ABDC. Note that the contribution of the DMF fragment with *m*/*z* = 30 is the same for all materials of the series and can be subtracted using the other DMF signals (*m*/*z* = 73 and 42) as a reference. The increasing intensity of the NO signal for the series from 0 to 50% (top) and 50 to 90% (bottom) of ABDC is depicted in Figure 7. The inset of Figure 7 (bottom) indicates that the integral intensity of *m*/*z* = 30 during the decomposition is linearly increasing from 0 to 50%, i.e. in the range where phase-pure MIXMOF materials can be obtained. The further steep increase in the range 50 to 90% is in accordance with the observations from DTG and also XRD. Obviously, at these higher ABDC contents additional amorphous phases are built instead of pure MIXMOFs.

The Langmuir surface area of the pure MOF-5 was determined to be 1250 m^2/g, whereas the 20 and 40% MIXMOFs had a decreased surface area of ca. 800 m^2/g. The decrease of the surface area is in accordance with the incorporation of ABDC molecules, which possess additional side groups that reduce the total accessible pore volume. Although the surface area that could be measured was significantly lower than that reported by Yaghi for MOF-5 single crystals,[50] the data obtained are in the same range than those from other literature reports (especially when a large amount of material was synthesized for catalytic applications).[18,51]

Catalytic Tests

Based on the results presented up to now we concluded that our mixed-linker metal-organic frameworks with an ABDC content from 0 to 40% represent robust, thermally stable and well-defined materials in which the number of active NH_2 side groups can be tuned using the desired ratio of BDC and ABDC, while undesired additional phases are formed in the presence of high ABDC concentrations (50 to 90%). Consequently, we have chosen the 40% MIXMOF $Zn_4O(BDC)_{1.8}(ABDC)_{1.2}$ (i.e. the phase pure material with the highest ABDC content) as the standard catalyst to screen for optimized reaction conditions. Typically 100 mg of the catalyst was used in the catalytic tests, which corresponds approximately to 0.05 mol-% of amino groups (based on PO). Due to the fact that propylene oxide is highly volatile (b.p. 34 °C) it cannot be excluded that remaining substrate is removed together with CO_2 during decompression after reaction. Therefore the yield of propylene carbonate is presented in all Figures and Tables instead of PO conversion. Note that no other products were detected by GC analysis.

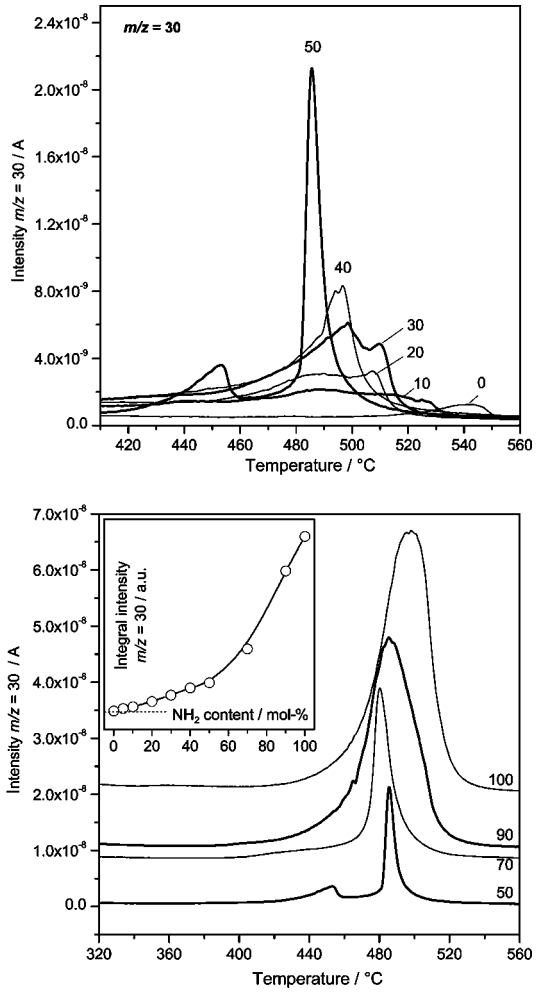

Figure 7. Characterization of the amount of NH_2 groups in the MIXMOF series via evaluation of the intensities of MS signals of NO (m/z = 30) which is formed by oxidation of NH_2 groups during decomposition. Top: series from 0 to 50% ABDC; bottom: series from 50 to 100%; the inset presents integral intensities of the NO signal as a function of the molar NH_2 content.

Figure 8 visualizes the influence of the CO_2 concentration (left) and reaction temperature (right) on the test reaction. Carbon dioxide was dosed to the reactor system via a mass flow controller allowing an accurate addition of the reactant. The highest activity was obtained using 2.2 equiv. (based on PO) of CO_2 (27 g) resulting in a propylene carbonate (PC) yield of 63% while both lower (1.4 equiv.; 18 g) and higher concentrations from 4.3 equiv. (54 g) to 10.7 equiv. (135 g) caused a significant decrease in activity (Figure 8, left). In the presence of 1.4 equiv. of CO_2 a pressure of ca. 30 bar was observed at the reaction temperature of 140 °C which suggests a gas phase reaction or a low solubility of gaseous carbon dioxide in propylene oxide. In contrast, increasing the CO_2 concentration to 2.2 equiv. caused its liquefaction (at ca. 50 bar) and the presence of a two-phase mixture with higher solubility of PO in CO_2 or the formation of an expanded liquid phase. Further increase of the CO_2/PO ratio led to increasing pressure in the system (ca. 80, 90, 125 and 145 bar for the four higher concentrations in Figure 8, left) above the critical pressure of carbon dioxide which obviously was not beneficial for the catalytic system. The observed maximum for a carbon dioxide excess of ca. 2.2 equiv. is in good accordance to literature reports on similar systems.[52–54] The optimized CO_2 concentration was tested at different reaction temperatures. No significant product formation was observed at temperatures of 80 °C or lower. Starting from 100 °C (PC yield: 36%) a more or less linear increase of the product yield was observed resulting in 52, 63 and 89% of PC at reaction temperatures of 120, 140 and 160 °C, respectively (Figure 8, right), which is also in accordance to literature data.[55]

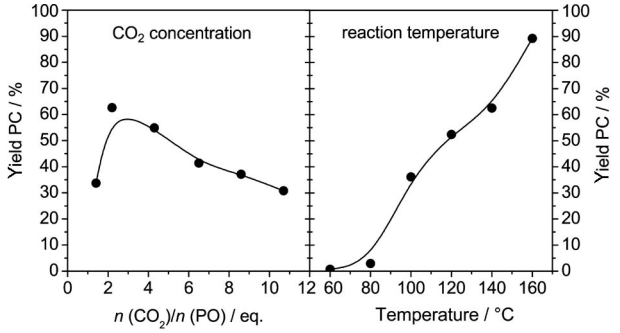

Figure 8. Influence of the reaction parameters on the PC yield; left: CO_2 concentration; conditions: 285 mmol propylene oxide, 0.1 mmol NEt_4Br, 0.127 mmol 40% MIXMOF, 1 mL of *tert*-butylbenzene as internal standard, 140 °C, 3 h; right: reaction temperature; conditions: 285 mmol propylene oxide, 615 mmol CO_2, 0.1 mmol NEt_4Br, 0.127 mmol 40% MIXMOF, 1 mL of *tert*-butylbenzene as internal standard, 3 h.

In the following experiments 2.2 equiv. of CO_2 and a reaction temperature of 140 °C were chosen as standard reaction conditions in order to study the influence of tetraalkylammonium halides NR_4X (Figure 9), which are commonly used promoters in the test reaction. As a blind test revealed, almost no PC formation is observed in the presence of pure MIXMOF (without additional NR_4X; Table 1, entry 1). In contrast, 22% of PC could be obtained when only NEt_4Br (and no MIXMOF) was added to the reaction mixture (Table 1, entry 3). However, the combination of 40% MIXMOF and NEt_4Br resulted in an enhanced activity (PC yield: 63%). Comparison of different NR_4X additives (R = Et, Bu; X = Cl, Br, I) shows a clearly less pronounced influence of the alkyl group compared to the halide anion (Figure 9). Both chloride salts (NEt_4Cl and NBu_4Cl) led only to 20 and 21% of PC yield, respectively, while the product yield was doubled in the presence of the corresponding iodides (NEt_4I: 44%, NBu_4I: 40%). Highest activity was observed using the bromides (NEt_4Br: 63%, NBu_4Br: 49%). The observed results are in contrast to literature reports in which iodides were found to be the best promoters (in accordance to the increasing nucleophilicity).[41,53] However, in the presence of microporous MIXMOFs the diffusion of the large iodide might be hampered, thus explaining the slightly reduced activity compared to the bromides.

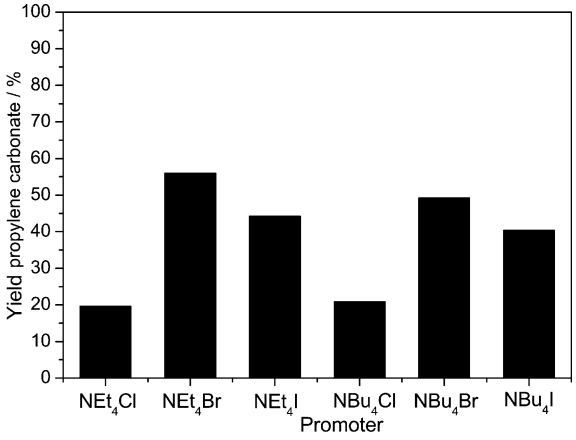

Figure 9. Various tetraalkylammonium halides as promoters; conditions: 285 mmol propylene oxide, 615 mmol CO_2, 0.1 mmol NR_4X, 0.127 mmol 40% MIXMOF, 1 mL of *tert*-butylbenzene as internal standard, 140 °C, 3 h.

Table 1. Reference tests; conditions: 285 mmol propylene oxide, 615 mmol CO_2, 140 °C, 3 h; homogeneously dissolved Zn^{2+}, H_2ABDC and H_2BDC were used in the same amount as present in the solid MIXMOF catalyst.

Entry	Catalyst	Molar amount of catalyst [mmol]	Additive	% Yield of propylene carbonate
1	MIXMOF	0.127 (Zn: 0.508; ABDC: 0.152; BDC: 0.229)	–	1
2	MIXMOF	0.127 (Zn: 0.508; ABDC: 0.152; BDC: 0.229)	NEt_4Br	63
3	–	–	NEt_4Br	22
4	$Zn(OAc)_2$	0.508	NEt_4Br	34
5	H_2ABDC	0.152	NEt_4Br	42
6	$Zn(OAc)_2$ + H_2ABDC	Zn: 0.508; ABDC: 0.152	NEt_4Br	66
7[a]	$Zn(OAc)_2$ + H_2ABDC + H_2BDC	Zn: 0.508; ABDC: 0.152; BDC: 0.229	NEt_4Br	72
8[b]	$Zn(OAc)_2$ + H_2ABDC + H_2BDC	Zn: 0.102; ABDC: 0.030; BDC: 0.046	NEt_4Br	31

[a] Simulating a completely dissolved MIXMOF. [b] Simulating a MIXMOF, which is dissolved to 20%.

To answer the question whether the reaction was really catalyzed by the solid MIXMOF catalyst or by partially dissolved Zn ions or linker molecules we performed the test reaction under standard conditions using Zn acetate and 2-aminobenzene-1,4-dicarboxylic acid (H_2ABDC), respectively, as the catalyst (Table 1, entries 4 and 5). The molar amounts of Zn and H_2ABDC were the same as in the solid 40% MIXMOF. However, the amount of PC found after the reaction (Zn acetate: 34%; H_2ABDC: 42%) was clearly lower than the 40% MIXMOF catalyst (63%). Only when we used combinations of $Zn(OAc)_2$ and H_2ABDC higher PC yields could be obtained. A mixture of $Zn(OAc)_2$ and H_2ABDC resulted in 66% of PC (Table 1, entry 6), whereas even 72% (Table 1, entry 7) were obtained when we used a mixture of $Zn(OAc)_2$, H_2ABDC and H_2BDC (which simulates a completely dissolved 40% MIXMOF). However, it might be possible that in this case the basic acetate groups from the Zn precursor acted as nucleophilic groups for the activation of the epoxide and thus contributed to some extent to the catalytic performance.[34] Due to their high catalytic activity (which is comparable to the homogeneously dissolved building blocks), solid MIXMOF catalysts seem to be suitable for continuous flow applications, where their advantage over homogeneous systems should become even more evident.

Obviously, the solid MIXMOF is almost as active as its dissolved building blocks in the same stoichiometric amount as present in the MIXMOF (compare entries 2 and 7 in Table 1). An additional control experiment where we simulated the dissolution of 20% of the MIXMOF catalyst (Table 2, entry 8), showed only 50% of the activity as in the presence of the solid catalyst. Consequently, we can exclude the possibility that partially dissolved species were (sole) active species. If this were the case, the solid material would have to be dissolved completely to obtain the same product yield. However, the solid catalyst could be filtered off after the reaction and recycled at least twice (Table 2). Because of the very specific reaction conditions that are necessary for the MOF synthesis it is highly improbable that the material was completely dissolved during the reaction and rebuilt at the end.

Table 2. Repetitive use of the catalyst. Reaction conditions: 285 mmol propylene oxide, 615 mmol CO_2, 0.127 mmol 40% MIXMOF, 0.1 mmol NEt_4Br, 140 °C, 3 h; after each run the catalyst was washed using diethyl ether and fresh NEt_4Br was added in the subsequent reaction.

Entry	Run	% Yield of propylene carbonate
1	first	63
2	second	45
3	third	41

The results of the recycling experiments are summarized in Table 2 and Figure 10. The decrease in product yield from 63 to 45 and 41% in the second and third run (Table 2) might be explained by the fact that the MIXMOF catalyst was only rinsed with diethyl ether after each run, and no special reactivation procedures were applied. Nevertheless the main reflections of the MIXMOF were still present in the powder X-ray diffraction pattern of the material after the third catalytic cycle (Figure 10). In spite of the decreased activity after the first run, almost no additional drop in product yield was observed after the second run. This stands in contrast to literature reports in which an exponential decrease has been observed upon reuse.[34]

The presented results indicate that our standard material 40% MIXMOF is a suitable catalyst for propylene carbonate synthesis from propylene oxide and carbon dioxide. Most probably the activation of the substrate molecules takes place at the amino side groups of the material which is in accordance with literature reports on amine-functionalized SBA-15 materials. On the other hand, the Zn ions in the framework structure are coordinatively saturated; there-

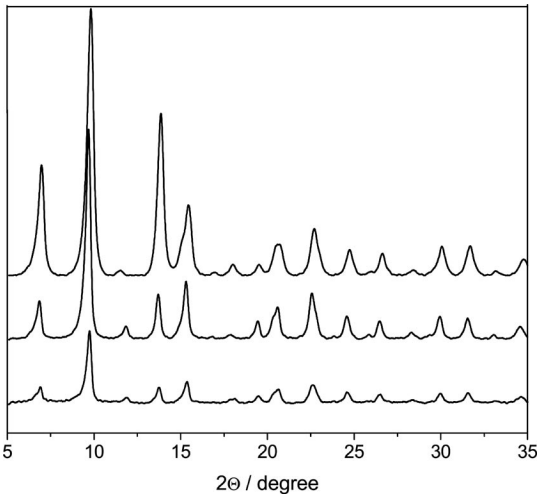

Figure 10. X-ray powder diffraction patterns of freshly prepared (top) 40% MIXMOF and the same material after one (middle) and three (bottom) catalytic cycles.

fore they should not be accessible for substrate coordination. On basis of this hypothesis we expect that the catalytic activity of the MIXMOF series should increase with the content of ABDC.

The experimental data presented in Figure 11 indicate that this is indeed the case. While the PC yield with pure MOF-5 (0% ABDC) amounted to only 44%, it could be stepwise increased up to 63% with 40% MIXMOF. Based on the total ABDC concentration of ca. 0.05 mol-%, a turnover number (TON) of 1180 can be calculated for catalytically active amino groups, which corresponds to a turnover frequency (TOF) of about 400 h^{-1}. The reaction time of three hours was comparatively short compared to literature reports on metal oxide based catalysts, where generally longer reaction times (8–24 h) have to be applied to obtain a comparable product yield. A better catalytic performance within three hours has up to now only been reported in the presence of immobilized transition metal complexes.[56] In

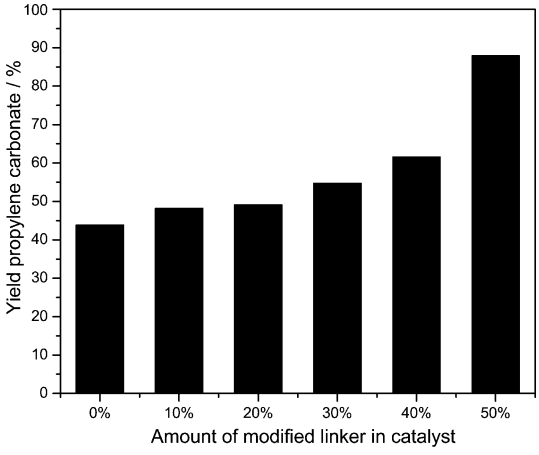

Figure 11. Influence of ABDC content on the catalytic performance; conditions: 285 mmol propylene oxide, 615 mmol CO_2, 0.1 mmol NEt_4Br, 0.127 mmol MIXMOF, 1 mL of *tert*-butylbenzene as internal standard, 140 °C, 3 h.

contrast to these systems, however, the MIXMOF catalysts do not require the use of additional transition metals (except of the Zn from the framework). Furthermore, no costly, complicated or time-consuming synthesis of the transition metal complexes is required for the MIXMOFs.

Due to the fact that also pure MOF-5 (0% of ABDC) catalyzes the reaction (although it does not contain NH_2 groups), we speculate that also partially unsaturated Zn species at the surface of the framework might have been accessible for substrate activation. However, higher amount of basic NH_2 sites led to an increased activity of the resulting catalysts. Beside the possible formation of carbamic acid via the activation of carbon dioxide,[49,55] also a base catalyzed ring opening of the epoxide might be possible.[57] Spectroscopic studies to elucidate the underlying reaction mechanism are currently underway.

Conclusions

Using optimized reaction conditions a series of MOF-5 based mixed-linker metal-organic frameworks (MIXMOFs) could be synthesized in which the benzene-1,4-dicarboxylate (BDC) linkers have been partially replaced by functionalized 2-aminobenzene-1,4-dicarboxylate (ABDC). X-ray powder diffraction and TG/MS analysis proved the presence of pure MIXMOFs up to an ABDC content of 40% while additional undesired phases might be formed at higher ABDC concentration. The presence of MIXMOFs (instead of a mechanical mixture of MOF-5 and IRMOF-3) was proven by high-resolution X-ray diffraction and DTG. The amount of amino groups, which represent accessible basic sites for catalytic applications, can be tuned by choosing the appropriate BDC/ABDC ratio. Although the thermal stability of the materials in air is decreasing with increasing degree of substitution from 450 °C (pure MOF-5, 0% of ABDC) to ca. 350 °C (40% MIXMOF), the resulting MIXMOFs are suitable catalysts for applications in the temperature range at least up to 300 °C. This is successfully demonstrated using the formation of propylene carbonate (PC) via insertion of carbon dioxide into propylene oxide (PO) as a test reaction. In combination with NR_4X additives solid MIXMOF catalysts show catalytic activities that are comparable to those observed for their homogeneously dissolved building blocks (Zn salts, H_2BDC, H_2ABDC) and they can be recycled several times with only moderate loss in activity. A comparison of the different materials of the MIXMOF series clearly indicates a dependence of activity on the amount of amino groups in the material. Due to the fact that pure MOF-5 (without NH_2 groups) also catalyzes the reaction, the activation of the substrates takes most probably place both at the basic amino groups and at accessible Zn centers at the surface (free coordination sites). In summary, the MIXMOFs presented in this work may represent a promising new class of catalyst for propylene carbonate synthesis and related base-catalyzed reactions.

Experimental Section

Synthesis of Mixed-Linker Metal-Organic Frameworks: The standard material 40% MIXMOF was synthesized as follows: $Zn(NO_3)_2 \cdot 6H_2O$ (5.950 g, 20 mmol), benzene-1,4-dicarboxylic acid (1.495 g, 9 mmol) and 2-aminobenzene-1,4-dicarboxylic acid (1.087 g, 6 mmol) were dissolved in 500 mL of *N*,*N*-dimethylformamide (DMF) at room temp. The mixture was put in a preheated oil bath at a reaction temperature of 150 °C for 18 h. The resulting yellowish brown precipitate was filtered off and washed five times with 50 mL of DMF each. Physically adsorbed solvent was then removed in vacuo at 80 °C for 5 h. Before using the material in the test reaction, the predried MIXMOF was calcined in air at 250 °C for 4 h to remove the solvent from the pores. All other materials were synthesized accordingly using the appropriate ratio of BDC and ABDC.

Material Characterization: Powder X-ray diffraction patterns were recorded on a Siemens D5000 diffractometer equipped with a Ni filter using Cu-K_α radiation. Measurements were performed in the 2Θ range from 5 to 55° with a step size of 0.01° and a step time of 2 s. Peak positions were adjusted using a copper plate as the reference [Cu (111) peak at 43.3°]. High-resolution powder X-ray diffraction patterns were recorded at beamline BM01B (ESRF Grenoble) using synchrotron X-ray radiation (wavelength: 0.49896 Å). Scanning electron microscopy was performed with a Gemini 1530 field emission microscope (Zeiss). The samples were investigated as prepared at low voltage (U = 1 kV). Thermoanalytical (TA) and mass spectrometric (MS) experiments were carried out isothermally or non-isothermally (heating rates were generally in the range of 5–10 K min^{-1}) on a Netzsch STA 409 simultaneous thermal analyzer equipped with a gas pulse device enabling injection of a certain amount of two different pure gases or gaseous mixtures into the system. The amount of injected gas could be varied from 0.01 to 10 mL; primarily, volumes of 1.0 and 2.0 mL were used.

Gases evolved during reaction and/or injected into the system were monitored on-line using a Omnistar (Pfeiffer Vacuum) quadrupole mass spectrometer, connected to the thermal analyzer by a heated (ca. 200 °C) stainless steel capillary. The determination of the thermal stability of the MOFs was carried out in an atmosphere of 20 vol.-% O_2, balance He, using a total gas flow of 50 mL min^{-1}.

Catalytic Tests: The catalytic reactions were performed in a 500 mL high pressure stainless-steel autoclave (Medimex No. 128) equipped with an efficient heating and cooling system. The quantity of liquid CO_2 was measured by a RHEONIK mass flow controller (RHM 01, RHE 02). Stirring was done by a motor of type EMOD EEDF 56L/2A equipped with a magnetic-coupled gas stirrer. The stirring rate was set at 1000 rpm. In a typical reaction, propylene oxide (285 mmol), the MIXMOF (0.127 mmol) and the NR_4X (0.1 mmol) were filled into the reactor. *tert*-Butylbenzene (1 mL) was added as an internal standard for GC analysis. A defined amount of carbon dioxide (PANGAS, 99.995%) from a liquid-CO_2 gas cylinder equipped with a dip tube was then dosed into the reactor by employing a compressor (NWA PM-101), and heating and stirring were started. After having reached the working temperature (normally 140 °C), the reaction proceeded for 3 h, then rapid cooling down to room temperature was initiated by a water flow system. After reaching room temperature, the CO_2 pressure was released by opening the outlet valve. This decompression was carried out slowly during half an hour, in order to minimize the loss of reaction mixture and to allow the liquid phase to degas properly. After opening the reactor, the reaction mixture was analyzed by a gas chromatograph (Thermoquest Trace GC, CE Instruments) equipped with a HP-FFAP capillary column (30 m × 0.32 mm × 0.25 μm) and a flame ionization detector (FID).

Safety Note: The experiments described in this paper involve the use of high pressure and require equipment with an appropriate pressure rating.

Supporting Information (see also the footnote on the first page of this article): DTG data of a mechanical mixture of MOF-5 and the material with 100% of ABDC in comparison to a real MIXMOF and Raman spectra of the MIXMOF series.

Acknowledgments

The authors thank the Swiss-Norwegian Beamline (SNBL) at the European Synchrotron Radiation Facility (ESRF) in Grenoble for providing beamtime and Wouter van Beek for supporting the high-resolution XRD measurements, Dr. Frank Krumeich and the EMEZ (Electron Microscopy ETH Zurich) are acknowledged for microscope time and recording of SEM pictures, as well as Dr. Andrew D. Burrows and Laura Fisher (University of Bath) for performing the surface area measurements.

[1] U. Mueller, M. Schubert, F. Teich, H. Puetter, K. Schierle-Arndt, J. Pastré, *J. Mater. Chem.* **2006**, *16*, 626–636.
[2] M. Eddaoudi, J. Kim, N. Rosi, D. Vodak, J. Wachter, M. O'Keeffe, M. Yaghi Omar, *Science* **2002**, *295*, 469–472.
[3] O. M. Yaghi, M. O'Keeffe, N. W. Ockwig, H. K. Chae, M. Eddaoudi, J. Kim, *Nature* **2003**, *423*, 705–714.
[4] S. Kitagawa, R. Kitaura, S. Noro, *Angew. Chem. Int. Ed.* **2004**, *43*, 2334–2375.
[5] A. K. Cheetham, C. N. R. Rao, R. K. Feller, *Chem. Commun.* **2006**, 4780–4795.
[6] G. Férey, *Chem. Soc. Rev.* **2008**, *37*, 191–214.
[7] T. Düren, L. Sarkisov, O. M. Yaghi, R. Q. Snurr, *Langmuir* **2004**, *20*, 2683–2689.
[8] J. L. C. Rowsell, O. M. Yaghi, *Angew. Chem. Int. Ed.* **2005**, *44*, 4670–4679.
[9] H. Frost, T. Düren, R. Q. Snurr, *J. Phys. Chem. B* **2006**, *110*, 9565–9570.
[10] E. Biemmi, C. Scherb, T. Bein, *J. Am. Chem. Soc.* **2007**, *129*, 8054–8055.
[11] W. J. Rieter, K. M. L. Taylor, W. Lin, *J. Am. Chem. Soc.* **2007**, *129*, 9852–9853.
[12] K. Schlichte, T. Kratzke, S. Kaskel, *Microporous Mesoporous Mater.* **2004**, *73*, 81–88.
[13] S. S. Y. Chui, S. M.-F. Lo, J. P. H. Charmant, A. G. Orpen, I. D. Williams, *Science* **1999**, *283*, 1148–1150.
[14] U. Müller, M. M. Schubert, O. M. Yaghi in *Chemistry and Applications of Porous Metal-Organic Frameworks*, vol. 1 (Eds.: G. Ertl, H. Knözinger, F. Schüth, J. Weitkamp), Wiley-VCH, Weinheim, Germany, **2008**, pp. 247–262.
[15] L. Alaerts, E. Séguin, H. Poelman, F. Thibault-Starzyk, P. A. Jacobs, D. E. De Vos, *Chem. Eur. J.* **2006**, *12*, 7353–7363.
[16] F. X. Llabres i Xamena, A. Abad, A. Corma, H. Garcia, *J. Catal.* **2007**, *250*, 294–298.
[17] M. Sabo, A. Henschel, H. Fröde, E. Klemm, S. Kaskel, *J. Mater. Chem.* **2007**, *17*, 3827–3832.
[18] S. Hermes, M.-K. Schröter, R. Schmid, L. Khodeir, M. Muhler, A. Tissler, R. W. Fischer, R. A. Fischer, *Angew. Chem. Int. Ed.* **2005**, *44*, 6237–6241.
[19] S. Hermes, F. Schröder, S. Amirjalayer, R. Schmid, R. A. Fischer, *J. Mater. Chem.* **2006**, *16*, 2464–2472.
[20] Z. Wang, S. M. Cohen, *J. Am. Chem. Soc.* **2007**, *129*, 12368–12369.
[21] Z. Wang, S. M. Cohen, *Angew. Chem. Int. Ed.* **2008**, *47*, 4699–4702.
[22] K. K. Tanabe, Z. Wang, S. M. Cohen, *J. Am. Chem. Soc.* **2008**, *130*, 8508–8517.

[23] C.-D. Wu, A. Hu, L. Zhang, W. Lin, *J. Am. Chem. Soc.* **2005**, *127*, 8940–8941.
[24] S.-H. Cho, B. Ma, S. T. Nguyen, J. T. Hupp, T. E. Albrecht-Schmitt, *Chem. Commun.* **2006**, 2563–2565.
[25] K. C. Szeto, K. P. Lillerud, M. Tilset, M. Bjørgen, C. Prestipino, A. Zecchina, C. Lamberti, S. Bordiga, *J. Phys. Chem. B* **2006**, *110*, 21509–21520.
[26] K. C. Szeto, C. Prestipino, C. Lamberti, A. Zecchina, S. Bordiga, M. Bjørgen, M. Tilset, K. P. Lillerud, *Chem. Mater.* **2007**, *19*, 211–220.
[27] A. D. Burrows, C. G. Frost, M. F. Mahon, C. Richardson, *Angew. Chem. Int. Ed.* **2008**, *47*, 8482–8486.
[28] D. J. Darensbourg, M. W. Holtcamp, *Coord. Chem. Rev.* **1996**, *153*, 155–174.
[29] T. Sakakura, J.-C. Choi, H. Yasuda, *Chem. Rev.* **2007**, *107*, 2365–2387.
[30] M. Ramin, F. Jutz, J.-D. Grunwaldt, A. Baiker, *J. Mol. Catal. A* **2005**, *242*, 32–39.
[31] Y.-M. Shen, W.-L. Duan, M. Shi, *J. Org. Chem.* **2003**, *68*, 1559–1562.
[32] X.-B. Lu, B. Liang, Y.-J. Zhang, Y.-Z. Tian, Y.-M. Wang, C.-X. Bai, H. Wang, R. Zhang, *J. Am. Chem. Soc.* **2004**, *126*, 3732–3733.
[33] F. Li, L. Xia, W. Sun, G. Chen, *Chem. Commun.* **2003**, 2042–2043.
[34] M. Ramin, J.-D. Grunwaldt, A. Baiker, *J. Catal.* **2005**, *234*, 256–267.
[35] K. Kasuga, N. Kabata, T. Kato, T. Sugimori, M. Handa, *Inorg. Chim. Acta* **1998**, *278*, 223–225.
[36] D. Ji, X. Lu, R. He, *Appl. Catal. A* **2000**, *203*, 329–333.
[37] H. Jing, S. K. Edulji, J. M. Gibbs, C. L. Stern, H. Zhou, S. T. Nguyen, *Inorg. Chem.* **2004**, *43*, 4315–4327.
[38] X.-B. Lu, Y.-J. Zhang, B. Liang, X. Li, H. Wang, *J. Mol. Catal. A* **2004**, *210*, 31–34.
[39] X.-B. Lu, X.-Y. Feng, R. He, *Appl. Catal. A* **2002**, *234*, 25–33.
[40] H. Kawanami, A. Sasaki, K. Matsui, Y. Ikushima, *Chem. Commun.* **2003**, 896–897.
[41] J. Sun, S. Fujita, F. Zhao, M. Arai, *Green Chem.* **2004**, *6*, 613–616.
[42] J. Sun, S. Fujita, M. Arai, *J. Organomet. Chem.* **2005**, *690*, 3490–3497.
[43] M. Alvaro, C. Baleizao, D. Das, E. Carbonell, H. Garcia, *J. Catal.* **2004**, *228*, 254–258.
[44] M. Alvaro, C. Baleizao, E. Carbonell, M. El Ghoul, H. Garcia, B. Gigante, *Tetrahedron* **2005**, *61*, 12131–12139.
[45] M. Ramin, N. van Vegten, J.-D. Grunwaldt, A. Baiker, *J. Mol. Catal. A* **2006**, *258*, 165–171.
[46] T. Yano, H. Matsui, T. Koike, H. Ishiguro, H. Fujihara, M. Yoshihara, T. Maeshima, *Chem. Commun.* **1997**, 1129–1130.
[47] R. Srivastava, D. Srinivas, P. Ratnasamy, *Tetrahedron Lett.* **2006**, *47*, 4213–4217.
[48] M. Tu, R. J. Davis, *J. Catal.* **2001**, *199*, 85–91.
[49] R. Srivastava, D. Srinivas, P. Ratnasamy, *Microporous Mesoporous Mater.* **2006**, *90*, 314–326.
[50] H. Li, M. Eddaoudi, M. O'Keeffe, O. M. Yaghi, *Nature* **1999**, *402*, 276–279.
[51] S. Opelt, S. Türk, E. Dietzsch, A. Henschel, S. Kaskel, E. Klemm, *Catal. Commun.* **2008**, *9*, 1286–1290.
[52] M. Ramin, J.-D. Grunwaldt, A. Baiker, *Appl. Catal. A* **2006**, *305*, 46–53.
[53] F. Jutz, J.-D. Grunwaldt, A. Baiker, *J. Mol. Catal. A* **2008**, *279*, 94–103.
[54] S.-S. Wu, X.-W. Zhang, W.-L. Dai, S.-F. Yin, W.-S. Li, Y.-Q. Ren, C.-T. Au, *Appl. Catal. A* **2008**, *341*, 106–111.
[55] R. Srivastava, D. Srinivas, P. Ratnasamy, *Catal. Lett.* **2003**, *91*, 133–139.
[56] T. Sakakura, K. Kohno, *Chem. Commun.* **2009**, 1312–1330.
[57] G. J. Buist, J. M. Barton, B. J. Howlin, J. R. Jones, M. J. Parker, *J. Mater. Chem.* **1995**, *5*, 213–217.

Received: June 8, 2009
Published Online: July 20, 2009

